Femtosecond laser nanoaxotomy lab-on-a-chip for *in vivo* nerve regeneration studies

Samuel X Guo[1], Frederic Bourgeois[1], Trushal Chokshi[2], Nicholas J Durr[1], Massimo A Hilliard[3], Nikos Chronis[2] & Adela Ben-Yakar[1]

A thorough understanding of nerve regeneration in *Caenorhabditis elegans* requires performing femtosecond laser nanoaxotomy while minimally affecting the worm. We present a microfluidic device that fulfills such criteria and can easily be automated to enable high-throughput genetic and pharmacological screenings. Using the 'nanoaxotomy' chip, we discovered that axonal regeneration occurs much faster than previously described, and notably, the distal fragment of the severed axon regrows in the absence of anesthetics.

The understanding of the biological mechanisms of nerve regeneration and degeneration after injury holds the key to developing new therapies for human neurodegenerative diseases. These processes can be studied in model organisms by severing axons in a controlled manner and then observing their regrowth and functional recovery. The nematode *C. elegans* became ideal for such studies when the feasibility of *in vivo* axotomy was recently demonstrated using ultrafast laser pulses[1]. However, the side effects that the chemicals used to immobilize the worms for laser nanoaxotomy might have on nerve regeneration are difficult to evaluate unless nanosurgery can be performed *in vivo* without anesthetics. To minimize undesirable environmental effects during surgery and monitoring, we designed a microfluidic device that allows us to sever axons in *C. elegans* using ultrashort laser pulses with the same high precision as we demonstrated previously[1,2] while monitoring the subsequent axonal regeneration activity.

Several microfluidic devices and microelectromechanical systems (MEMS) have recently been developed for *C. elegans* including Petri dish–based microfluidics[3], microfluidic traps[4–6], a compact disc–based centrifugal device[7], a shadow imaging platform[8], microfluidic maze structures[7,9], a cantilever force MEMS sensor[10] and a platform to capture and sort worms[11]. But no demonstration of nanosurgery on a chip has been reported so far.

The integrated microfluidic device we designed has several unique features that are critical for the success of *in vivo* nerve regeneration studies: the worms are held directly against the glass cover for ideal focusing and precise nanosurgery; the trap is adjustable to the size of the worms, allowing immobilization of worms at various developmental stages (fourth larval (L4) to adult size); and the system integrates feeding modules and thus allows long-term follow-up studies of the axotomized worms as well as their sorting and screening.

The high-throughput microfluidic system integrates two separate modules: a trapping module for nanosurgery and time-lapse imaging, and a feeding module for recovery of the operated worms (**Fig. 1a**). Follow-up imaging of injured axons and their regrowth is performed using the same trapping module. Depending on the outcome of the imaging session, the worms can either be flushed out through the inlet or sorted into different feeding chambers according to their axonal recovery progress. If necessary, the feeding chambers can be connected to a supply of fresh liquid growth medium, allowing observations for an extended period of time. The whole cycle of loading, trapping and operating takes approximately 1 min per worm, compared to 10 min using nanoaxotomy on agar pads[1].

We adopted a two-layer microfluidic approach[12] that incorporates a thin membrane (~40 μm) between the layered channels (**Supplementary Methods** and **Supplementary Table 1** online). The worms are loaded in a 50-μm-deep and 110-μm-wide microfluidic channel in the bottom layer of the chip (**Fig. 1b,c**). Pressurization of the top layer results in the deflection of the membrane that quickly immobilizes the freely moving worm (**Supplementary Video 1** online). After the axons of the immobilized worm are severed, the pressure is released, and the worm is transferred to one of the feeding chambers.

Membrane deflection depends on the applied pressure in the air channel as well as the dimensions of the bottom channel. Using two-photon imaging (**Supplementary Methods**), we mapped the cross-sectional profile of the trapping channel and studied the deflection of the membrane at different pressures (**Fig. 1d**). As pressure increases in the top layer, the membrane begins deflecting downward, immobilizing the nematode by pressing it into one of the sides of the channel (**Fig. 1c,e**). We immobilized L4 and young adults using a minimal pressure of 110 kPa air. We performed a survival test on 20 worms: we trapped them with a pressure of 110 kPa for 60 min and monitored them for the subsequent 3 d. We did not observe any morphological and behavioral defects or premature death (**Table 1**, experimental set 5).

In the trapping module the side of the nematode lying against the cover glass is flattened (**Fig. 1e**). This flattening is optimal for both imaging and surgery because most of the length of the target axon is

[1]Department of Mechanical Engineering, The University of Texas at Austin, 204 E. Dean Keeton Street, Austin, Texas 78712, USA. [2]Department of Mechanical Engineering, University of Michigan, 2350 Hayward Street, Ann Arbor, Michigan 48109, USA. [3]Queensland Brain Institute, University of Queensland, Brisbane QLD 4072, Australia. Correspondence should be addressed to A.B. (ben-yakar@mail.utexas.edu).

RECEIVED 31 JANUARY; ACCEPTED 24 MARCH; PUBLISHED ONLINE 13 APRIL 2008; DOI:10.1038/NMETH.1203

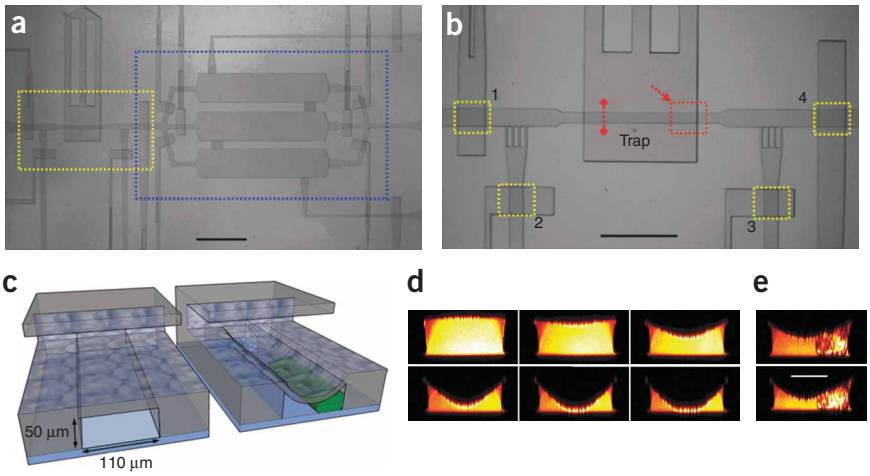

Figure 1 | The nanoaxotomy lab-on-a-chip. (**a**) Overview of the chip with the trap system (yellow rectangle) and three recovery chambers (blue rectangle). (**b**) Magnified view of the trapping system (yellow rectangle in **a**). Valves 1–4 (yellow rectangles) respectively control inlet regulation, fine positioning of the worm (2 and 3) and gating to the recovery chambers. (**c**) Conceptual three-dimensional section renderings of the bilayer trap channels without and with an immobilized worm. (**d**) Two-photon images of cross-sectional profiles of the microchannel in the trap area for increasing air pressures from 0 to 35, 70, 105, 140 and 175 kPa. (**e**) Cross-sectional two-photon images of a trapped worm at 105 and 140 kPa. Scale bars, 2 mm (**a**), 1 mm (**b**) and 50 µm (**e**).

in focus. This design provides an optical path from the objective lens to the axon inside the worm that is similar to the previous nanoaxotomy method on agar pads[1,2].

We performed nanosurgery of neuronal processes by a train of 200 highly focused 220-fs laser pulses of 7.2 nJ at 1 kHz repetition rate and 780-nm wavelength (**Supplementary Methods**, **Supplementary Fig. 1** and **Supplementary Video 2** online). We performed axotomies at one-third of the process length from cell body to axon branching (**Supplementary Fig. 2** online). For time-lapse imaging, we collected fluorescence images at approximately 10-min intervals (**Fig. 2**). Nerve regrowth was not continuous but occurred in bursts of elongation and retraction of filopodia that could be as fast as 2 µm in 10 s. Axons reconnected to their distal end within approximately 70 min after surgery.

To investigate whether the absence of anesthetics (phenoxypropanol or levamisole) during nanosurgery would increase the probability of successful axonal recovery (regrowth and reconnection), we performed four sets of experiments (**Table 1**, experimental sets 1–4). We first considered the effect of the growth medium on axonal recovery. Worms grown on agar and in CeRH liquid growth medium both showed similar axonal recovery rates. Considering the growth medium as the variable, the Fisher's exact test (**Supplementary Methods**) yielded probabilities of $P_{13} = 0.284$ for worms axotomized on agar pad and paralyzed with levamisole, $P_{24} = 0.328$ for worms axotomized in chip using the microfluidics trap and $P_{13–24} = 0.184$ regardless of the immobilization procedure. The change of the growth environment thus seems to have no statistical significance.

To characterize the statistical significance of the absence of anesthetics on nerve regeneration, we compared the results of experiments using different immobilization methods. Considering the immobilization procedure as the variable, the Fisher's exact test yields the following probabilities: $P_{12} = 0.146$, $P_{34} = 0.192$ and $P_{12–34} = 0.046$ for worms grown on agar, in CeRH liquid medium and regardless of the growth habitat, respectively. A probability of 0.046 indicates that as expected, anesthetics significantly slow down the nerve regeneration process and delay it by several hours[2].

Notably, in addition to regrowth of the proximal fragments, we also observed the distal fragments always sprouting growth cones. The regrowth of the distal fragment was already visible within a few minutes after axotomy, while it took at least 30 min for the proximal fragment to start regrowing. The regrowth velocity of both fragments was the same. The distal ends seemed to lack any kind of guidance and never reconnected to the proximal end. The regrowth of the distal end seemed to stop shortly after the proximal end began its regrowth. Furthermore, once the proximal growth cones reconnected to their distal ends, the growth cones from the distal ends did not recess (**Fig. 2b**). This result suggests that the microtubules within the distal end are stable and that actin, mitochondria and proteins necessary for the creation of a growth cone are present or might be transported from the remaining section of the process to its severed end. Because the cell body is missing and membranous vesicles cannot be fabricated, the mobility of the growth cone requires that these vesicles be endocytosed, transported and exocytosed at the forefront of the growth cone[13]. The hypodermal syncytium hyp7, enclosing the ALM and PLM neurons, is thought to provide a structural cue for the guidance of the proximal growth cones[14].

We also observed that axonal recovery does not depend on the location of the surgery along the process and even immediately

Table 1 | Summary of statistical observations

Set number	Growth medium	Surgery medium	Surgery on agar pad, paralyzed	Trapping on-a-chip	Surgery on-a-chip	Worm survival rate, 24 h	Axonal recovery time	Axonal recovery rate, 24 h	Worm survival rate, 72 h
1	Agar	Agar	+			20/20 (100%)	6–12 h	18/40 (45%)	18/20 (90%)
2	Agar	M9 buffer		+	+	20/20 (100%)	60–90 min	24/40 (60%)	20/20 (100%)
3	CeRH	Agar	+			20/20 (100%)	6–12 h	21/40 (53%)	20/20 (100%)
4	CeRH	CeRH		+	+	20/20 (100%)	60–90 min	26/40 (65%)	20/20 (100%)
5	CeRH	None		+		20/20 (100%)	N/A	N/A	20/20 (100%)

We performed nanoaxotomy and monitored the axonal recovery (regrowth and reconnection) of groups of 20 worms grown either on agar or in liquid growth medium (CeRH), and either paralyzed with a 0.2 µM solution of levamisole and operated on agar pads, or trapped in the new nanoaxotomy lab-on-a-chip device.

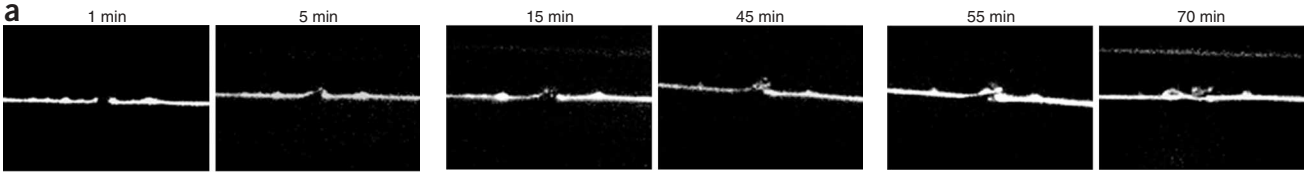

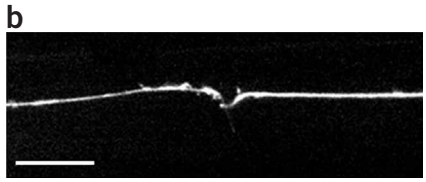

Figure 2 | Time-lapse imaging of axonal recovery on a chip. (**a**) Fluorescence images of an ALM neuron at the indicated times after the axotomy. Distal ends are on the left side of the pictures and proximal ends, on the right. After 5 min, the distal end displays a growth cone that is visible above the proximal stump. At 15 min, the growth cone branches off into two. At 45 min, a third branch sprouts close to the distal stump. The other two growth cones are out of focus. At 55 min, the third branch recesses, and the first two branches develop into a broad growth cone. The proximal end starts regrowing. At 70 min, the proximal end regrew and reconnected to the distal end a bit further past the distal stump. (**b**) Fluorescence image of axonal recovery in a different axon 35 min after axotomy. The distal growth was misguided and developed sideways (pointing downward on the picture). The proximal end is regrowing toward the distal part. Scale bar, 10 μm.

distal to the axonal branch (**Supplementary Methods**, **Supplementary Fig. 3** and **Supplementary Table 2** online). Axonal recovery rates varied between 62% and 73% with no statistically significant difference ($P = 0.627$). In a recent study[15], others showed that there was no regeneration of a severed axon beyond the axonal branch (the "distal process" as named in ref. 15) unless the branch is cut to stimulate regrowth of the distal process. We also performed surgeries on the branch and on both branch and distal process, both in chip and on agar pads. We did not observe any axonal recovery of severed branches in agreement with previous results[15]. We concluded, however, that regeneration of the distal process occurs independently of whether the branch is cut or not.

Behavioral assays are a widespread method to ascertain function of specific neurons. We proved the reliability of the laser surgery by ablating the circumferential axons of the VD and DD motor neurons in the microfluidic device, and observed the shrinker phenotype during a behavioral assay. We also tested the behavioral output of worms after severing the ALM and PLM axons at various locations. In general, *C. elegans* respond with a clear backward movement to a light mechanical stimulus (light touch) applied on the anterior half of their body (ALM-mediated) and with a forward acceleration when the light touch is applied on the posterior half of the body (PLM-mediated). With axotomies performed on different sections of ALM and PLM processes, we found that the cell body as well as a large part of the process themselves are not essential for a behavioral response to occur. Worms responded well with no change in their behavior when (i) we cut ALM and PLM processes on one side only, (ii) we cut ALM and PLM processes on both sides, and (iii) we ablated cell bodies of both ALM and PLM pairs. In contrast, axotomy at the branch clearly impaired the mechanical response (**Supplementary Video 3** online). These results confirmed the dual axonal-dendritic nature of the mechanosensory processes and demonstrated the crucial function of the synaptic branch to generate the light-touch behavioral output.

The advantages of this microfluidic chip over the immobilization techniques previously used in studies of *C. elegans*, such as anesthesia on agar pads or glue, are: (i) the use of no chemicals other than the liquid growth medium to interfere with the physiological processes of the worms, possibly increasing nerve regeneration success, (ii) the adaptive deflection of the membrane allows the immobilization of the worms from L4 to adult size, (iii) the worms do not need a recovery period after surgery, permitting immediate behavioral study of the post-axotomy functionality, (iv) the sample population is well contained, and experiment conditions are easily reproducible because the trap for surgery and the environment for recovery are on the same chip and finally, (v) the design of the chip is simple enough to be adapted to other organisms or many other kinds of experiments, including ablation, irradiation, stimulation or simply observation, widening the possibilities of high-throughput biological investigations.

Note: Supplementary information is available on the Nature Methods website.

ACKNOWLEDGMENTS

We thank C. Bargmann and M. Goodman for valuable discussions. This work was supported by grants from the US National Institutes of Health (NS058646 and NS060129) and the National Science Foundation (BES-0548673).

AUTHOR CONTRIBUTIONS

N.C. and A.B. designed the device; T.C. fabricated the microfluidic chip; S.X.G. and N.D. performed two-photon microscopy; F.B., M.H. and A.B. analyzed data; S.X.G., F.B. and A.B. designed experiments; S.X.G. and F.B. performed experiments; F.B. and A.B. wrote the paper.

Published online at http://www.nature.com/naturemethods/
Reprints and permissions information is available online at http://npg.nature.com/reprintsandpermissions

1. Yanik, M.F. *et al. Nature* **432**, 822 (2004).
2. Bourgeois, F. & Ben-Yakar, A. *Opt. Exp.* **15**, 8521–8531 (2007).
3. Gray, J.M. *et al. Nature* **430**, 317–322 (2004).
4. Chronis, N., Zimmer, M. & Bargmann, C.I. *Nat. Methods* **4**, 727–731 (2007).
5. Chalasani, S.H. *et al. Nature* **450**, 63–70 (2007).
6. Hulme, S.E., Shevkoplyas, S.S., Apfeld, J., Fontana, W. & Whitesides, G.M. *Lab Chip* **7**, 1515–1523 (2007).
7. Kima, N., Dempsey, C.M., Zoval, J.V., Sze, J.Y. & Madoub, M.J. *Sens. Actuat. B* **122**, 511–518 (2007).
8. Lange, D., Storment, C.W., Conley, C.A. & Kovacs, G.T.A. *Sens. Actuat. B* **107**, 904–914 (2005).
9. Qin, J. & Wheeler, A.R. *Lab Chip* **7**, 186–192 (2007).
10. Park, S.J., Goodman, M.B. & Pruitt, B.L. *Proc. Natl. Acad. Sci. USA* **104**, 17376–17381 (2007).
11. Rohde, C.B., Zeng, F., Gonzalez-Rubio, R., Angel, M. & Yanik, M.F. *Proc. Natl. Acad. Sci. USA* **104**, 13891–13895 (2007).
12. Unger, M.A., Chou, H.P., Thorsen, T., Scherer, A. & Quake, S.R. *Science* **288**, 113–116 (2000).
13. Kandel, E.R., Schwartz, J.H. & Jessell, T.M. *Principles of Neural Science.* 4th edn. (McGraw-Hill Medical, New York, 2000).
14. Chalfie, M. *et al. J. Neurosci.* **5**, 956–964 (1985).
15. Wu, Z. *et al. Proc. Natl. Acad. Sci. USA* **104**, 15132–15137 (2007).